Inorg. Chem. **2006**, *45*, 6604–6611

Bi^{3+}/M^{2+} Oxyphosphate: A Continuous Series of Polycationic Species from the 1D Single Chain to the 2D Planes. Part 1: From HREM Images to Crystal-Structure Deduction

M. Huvé,* M. Colmont, and O. Mentré

UCCS, équipe de Chimie du Solide, UMR CNRS 8181, ENSC Lille−UST Lille, BP 90108, 59652 Villeneuve d'Ascq Cedex, France

Received March 1, 2006

This work deals with the crystal-structure deduction of new structural types of Bi^{3+}–M^{2+} oxyphosphates (M is a transition element) from HREM images. Previous studies showed the unequivocal attribution of particular HREM contrasts to the corresponding Bi/M/O-based polycationic species in similar materials. On this basis, the examination of isolated crystallites of polyphased samples led to new HREM contrasts assigned to new polycationic species in three new structural types. This helped us to solve one crystal structure, and the two other forms have been deduced through HREM image decoding. It helped to model the investigated materials from the structural point of view as well as the chemical one. The three assumed crystal structures are formed by polycationic ribbons, *n* tetrahedra wide, surrounded by PO_4 groups, as already encountered in these series of oxyphosphates. However, here we deal with the original *n*= 4–6 cases, whereas, up to this work, only the *n*= 1–3 ribbons have been reported. The greater size of ribbons is associated with particular structural modifications responsible for complex HREM contrasts. The validity of the proposed models is verified in Part 2 of this work.

Introduction

It has been shown that most of the compounds isolated in the $Bi_2O_3-MO-P_2O_5$ (M = Cu, Zn, Co, Cd, Mn...) systems have strong structural relationships based on the existence of infinite polycationic ribbons formed by the edge sharing of $O(Bi,M)_4$ tetrahedra. The ribbons are surrounded by isolated PO_4 groups and ordered along various arrangements depending on the structural type.[1] Within that frame, a series of new disordered structural types based on double (D) and triple (T) (two and three $O(Bi,M)_4$ tetrahedra wide, respectively) ribbons have been discovered.[2−13] Previous work has shown the essential contribution of transmission electron microscopy in the structural study of these new double Bi^{3+}/M^{2+} oxide phosphates.[14] Considering the close Bi/M/P compositions between the isolated compounds so far, and the subsequent multiphased samples obtained within the search for new materials, we have established a method that allows for the deduction of the structural type from the electron diffraction (ED)/high-resolution electron microscopy (HREM) investigation of one single crystallite. This method goes through the establishment of HREM image codes

* To whom correspondence should be addressed. E-mail: Marielle.Huve@ensc-lille.fr.

(1) Abraham, F.; Cousin, O.; Mentré, O.; Ketatni, M. *J. Solid State Chem.* **2003**, *167*, 168.
(2) Ketatni, M.; Huvé, M.; Abraham, F.; Mentré, O. *J. Solid State Chem.* **2002**, *172* (2), 327.
(3) Colmont, M.; Huvé, M.; Ketatni, M.; Abraham, F.; Mentré, O. *J. Solid State Chem.* **2003**, *176* (1), 221.
(4) Colmont, M.; Huvé, M.; Abraham, F.; Mentré, O. *J. Solid State Chem.* **2004**, *177* (11), 4149.
(5) Huang, J.; Gu, Q.; Sleight, A. W. *J. Solid State Chem.* **1993**, *105*, 599.
(6) Abraham, F.; Ketatni, M.; Mairesse, G.;. Mernari, B. *Eur. J. Solid State Chem.* **1994**, *31*, 313.
(7) Tancret, N. Ph.D. dissertation, Université des Sciences et Technologies de Lille, France, 1995.
(8) Mizrahi, A.; Wignacourt, J. P.; Steinfink, H. *J. Solid State Chem.* **1997**, *133*, 516.
(9) Mizrahi, A.; Wignacourt, J. P.; Drache, M.; Conflant, P. *J. Mater. Chem.* **1995**, *5*, 901.
(10) Ketatni, M.; Mernari, B.; Abraham, F.; Mentré, O. *J. Solid State Chem.* **2000**, *153*, 48.
(11) Giraud, S.; Mizrahi, A.; Drache, M.; Conflant, P.; Wignacourt, J. P..; Steinfink, H. *Solid State Sci.* **2001**, *3*, 593.
(12) Abraham, F.; Ketatni, M.; Mernari, B. *Adv. Mater. Res.* **1994**, *1* (2), 223−232.
(13) Xun, X.; Uma, S.; Yokochi A.; Sleight, A. W. *J. Solid State Chem.* **2002**, 167 (1), 245.
(14) Huvé, M.; Colmont, M.; Mentré, O. *Chem. Mater.* **2004**, *16* (13), 2628.

10.1021/ic060342r CCC: $33.50
Published on Web 07/25/2006

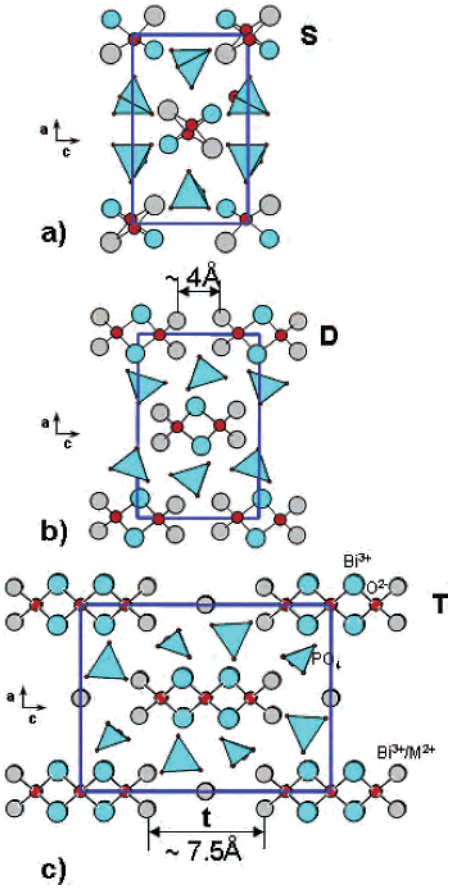

Figure 1. Projection along the *b* axis and evidence of (a) single chains (S) in $BiMPO_5$ (M = Mn, Co, Ni), (b) double ribbons (D) in BiM_2PO_6 (M = Cu, Co, Mn, Zn...), and (c) triple ribbons (T) in $Bi_{\sim 1.2}M_{\sim 1.2}PO_{5.5}$ (M = Zn, Co, Mn).

possible because of characteristic contrasts between Bi−M−O ribbons and surrounding PO_4 groups on HREM images; i.e., the parent compounds BiM_2XO_6[5−13] (which contain double ribbons) and $Bi_{\sim 1.2}M_{\sim 1.2}PO_{5.5}$[1] (which contains triple ribbons) revealed independent codes for D and T, respectively. The coexistence of both D and T in other structural types leads to the combination of the two codes on the HREM images and a possible deduction of the structural type and chemical formulation, confirmed afterward by the synthesis of a pure compound (powder and/or single crystal) and its X-ray diffraction (XRD) structural refinement. The latter was always in accordance with the structural model that proves the validity of the method.[2−4] This work is dedicated to the identification of three new oxide phosphates that contain the new $n = 4-6$ tetrahedra-wide ribbons. The structural modification effective for ribbons with $n > 3$ yields new contrasts/new codes. Their interpretation has been successfully interpreted in term of ribbon/PO_4 arrangement from HR images.

Experimental Section

The different $Bi_wM_xO_y(PO_4)_z$ oxides (M = Co, Cu, Cd) reported in this work have been prepared by heating stoechiometric mixtures of Bi_2O_3, MO, and $(NH_4)_2HPO_4$. The reactants are first dissolved in nitric acid and homogenized by stirring. A small amount of citric acid is added in order to complex and disperse the cations in the solution. The preparation is then heated at 150 °C up to complete water evaporation. The product is transferred to an alumina crucible. Several heating−grinding steps from 200 to 800 °C are applied for 72 h, and the final powder is quenched at room temperature.

Table 1. Sum-Up Table Showing Each Isolated Ribbon with Corresponding Nomenclature, Formulation, and Nomenclature Used for HREM

Polycations projected along *b*	Nomenclature, n surrounding PO_4	Formulation	Representation used for HREM
	S, 6	$[Bi_2M_2O_2]^{+5}$ *M* = Ni, Co, Mn	----
	D, 6	$[Bi_2M_4O_4]^{+6}$ *M* = Cu, Cd, Ca, Mn, Zn, Pb,	
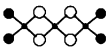	T, 8	$[Bi_{(8-x)}M_xO_6]^{+3(8-x)+2x}$ *M* = Cu, Co, Mn, Zn, Cd	
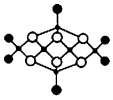	Q, 8	$Bi_{(12-x)}M_xO_{10}]^{+3(12-x)+2x}$ *M*= Cu, Cd	
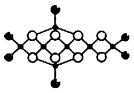	P, 10	$[Bi_{(14-x)}M_xO_{12}]^{+3(14-x)+2x}$ *M* = Cu, Cd	
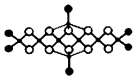	H, 12	$[Bi_{(16-x)}M_xO_{12}]^{+3(16-x)+2x}$ *M* = Cu, Cd	

Electron-diffraction patterns (EDP) were obtained on a JEOL 200CX and high-resolution images on a JEOL 4000EX transmission electron microscope with a point resolution of 1.7 Å. In each case, the materials have been crushed and dispersed on a holey carbon film deposited on a Cu grid. The computer-simulated HREM images were calculated using the JEMS program.[15]

State of the Art: Topological Relations between the Isolated Compounds. The polycationic species evidenced so far are shown in Figure 1, where S stands for single, D for double, and T for triple tetrahedra-wide ribbons. S exists in $BiMO(PO_4)$ (M = Mn, Ni, Co),[13,16,17] D in $BiM_2O_2(PO_4)$ (M = Ca, Cu, Zn, Mg, Pb...),[5−13] and T in $Bi_{\sim 1.2}M_{\sim 1.2}O_{1.5}(PO_4)$ (M = Mn, Co, Zn),[1] whereas D and T both coexist in the reported $Bi_{\sim 6.22}Cu_{\sim 6.2}O_8(PO_4)_5$,[2] $Bi_{\sim 3}Cd_{\sim 3.72}M_{\sim 1.28}O_5(PO_4)_3$ (M = Co, Cu, Zn),[3] and $Bi_{\sim 3.785}Cd_{\sim 3.575}Cu_{\sim 1.5O5.5}(PO_4)_{3.5}$[4] materials. The structural relationship between these oxides is determined on the basis of the ribbon arrangement isolated by PO_4 groups. The orthorhombic unit cell then shows the following similarities: the *b* (∼5.5 Å) parameter is intrinsic to the ribbon structure, i.e., the height of two edge-sharing tetrahedra, whereas *a* (∼11.5 Å) is twice the distance between the sheets of ribbons isolated by PO_4^{3-} rows (Figure 1). Of course, the *c* parameter is characteristic of the structural type, because it depends on the ribbon width and their arrangement. Along the *b* direction, the structures are approximately known and consist of infinite edge-shared tetrahedra ribbons. Consequently, a 2D [010] image is sufficient to construct a suitable model. That is why this work is especially focused on the [010] images.

Main Structural Rules Recall. The formulation of compounds that belong to a structural type can be deduced from the ribbon/PO_4 arrangement using empirical rules that have been proved valid for the totality of the prior cases and intensively discussed in ref 14.

The center of the ribbons is solely occupied by Bi^{3+}, whereas the edge holds either M^{2+} cations (leading to ordered materials such as $BiM_2O_2(PO_4)$) or mixed Bi^{3+}/M^{2+} cations (leading to disordered compounds such as $Bi_{\sim 1.2}M_{\sim 1.2}O_{1.5}(PO_4)$[1]).

The number of surrounding PO_4 is a function of the ribbon size; double and triple ribbons are in any case surrounded by six and eight phosphate groups, respectively.

In the disordered compounds, M^{2+}-containing tunnels coordinated by PO_4 corners are created between ribbons with available space (distance between the edges of the two ribbons ≈ 7.5 Å; Figure 1).

Accurate knowledge of the ribbon sequence in the (010) plane is then sufficient to locate PO_4 and tunnels from steric considerations. The formulation of a possible compositional range is then possible, considering the mixed Bi^{3+}/M^{2+} ratio at the edges of ribbons (fully occupied) and the partial M^{2+} filling of tunnels. For a general view of the nomenclature used below, the details of existing ribbonlike units are reported in the Table 1.

HREM Image Code for Double- and Triple-Ribbon-Containing Compounds. As reported in the Introduction and intensively developed in ref 14, the HREM investigation of the compounds described so far led to the establishment of an image code sufficient enough to locate both D and T in the unit cell. Briefly, the double (D) and triple (T) ribbons take place in the dark region between two white circlelike and crosslike motifs, respectively along *a*. The correspondence between calculated HREM contrasts and the structural motifs are shown in Figure 2 for a defocus of −10 nm and a thickness of 4.1 nm.

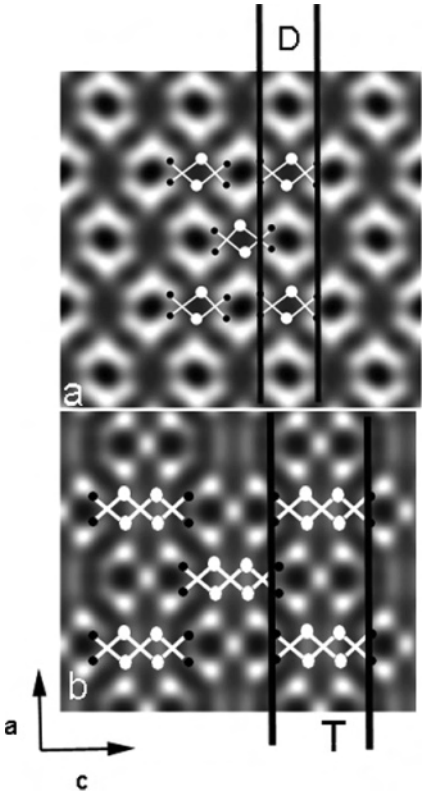

Figure 2. Image code: (a) simulated image (defocus = −10 nm, thickness = 4.1 nm) for BiM_2PO_6. The superposition of the projected ribbons (along *b*) shows that double chains are surrounded by four white circles along *c*; (b) simulated image (defocus = −10 nm, thickness = 4.3 nm) for $Bi_{\sim 1.2}M_{\sim 1.2}(PO_4)O_{1.5}$. The superposition of the triple ribbons (T) along *b* shows their location between white crosses. Their stacking along *a* is called a type T column.

Results and Discussion

Process. This current section deals with the crystal-structure deduction of compounds containing new kinds of ribbons with a width greater than 3 tetrahedra. The HREM studies have been performed on multiphased samples after measurements of original lattice parameters. The strategy used here is developed in three subsequent stages:

(a) The first investigated system deals with the HREM contrast observation and decoding of a pertinent phase with regard to its known crystal structure refined from single-crystal XRD patterns.[18]

(b) The code is applied to new observed contrasts, leading us to postulate new structural types and their mean chemical formulations.

(c) The synthesis of either single-crystal or pure materials is performed to help deduce the compositional range. The refined crystal structures that validate the HREM investigation are described in part 2 in this series.[18]

(A) HREM Investigation of the New Dtt/H Structural Type. In the frame of the $Bi_2O_3-MO-P_2O_5$ investigation,

(15) Stadelmann, P. *JEMS: Java version of Electron Microscopy Simulation*; 1999−2006.
(16) Nadir, S.; Swinnea, J. S.; Steinfink, H. *J. Solid State Chem. 148*, 295−301.
(17) Abraham, F.; Ketatni, M. *Eur. J. Solid State Inorg. Chem.* **1995**, *32*, 429−437.
(18) Colmont, M.; Huvé, M.; Mentré, O. *Inorg. Chem.* **2006**, *45*, 6612−6621.

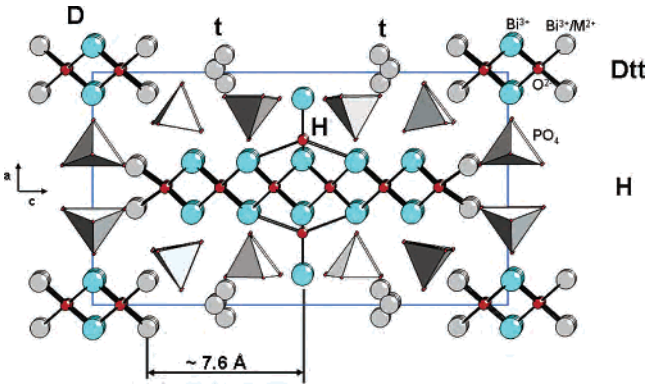

Figure 3. Projection along ⟨010⟩ of the Dtt/H structural type.

M = Cd, Cu, the sample corresponding to the nominal composition $BiCd_{0.29}Cu_{0.03}(PO_4)_{0.59}O_{0.93}$ shows an XRD powder pattern composed of at least two phases. The ED investigation has shown that the major one shows lattice parameters $a \approx 5.5$ Å, $b \approx 11.5$ Å, and $c \approx 21$ Å. The [010] zone axis pattern is compatible with a primitive Bravais lattice. It corresponds to the Dtt/H crystal structure type described in ref 18 that has been refined for a crystal with the $Bi_{15.32}Cd_{10}(PO_4)_{10}O_{18}$ composition.

The projection of the structure along <010> is shown on Figure 3. At this stage, one should remark the combination of tunnels (t), double ribbons (D) and sextuplet (H) ribbons within the Dtt/H sequence. This nomenclature first proposed in a previous work[14] describes tunnel/ribbon sequences along c at $x = 0$ and $x = 1/2$. Note the structural modification of H ribbons for which a OBi_5 pyramid is attached perpendicularly to the ribbon width. These 3D excrescences will be called "ribbon-fins" in the discussion to come. Also note that H ribbons are surrounded by 12 PO_4 groups in the a,c plane.

Image Code and Compound Formulation. The [010] HREM image of the Dtt/H structural type was simulated for a thickness of 4.3 nm and a defocus of 10 nm and compared with the experimental image, panels a and b of Figure 4. A projection of the structure is superimposed. The good matching between calculated and observed images validates the structural model used in this section. Double ribbons are then likely located in the D dark regions of column D, whereas the sextuplet ribbons take place in the dark region between two white ovals surrounded by chevrons headed in opposite directions along a, in column H. The latter is surrounded by 12 independent PO_4 tetrahedra. A chemical formulation range can be deduced from the a,c projection of the structure. It leads to $H_1D_1t_2(PO_4)_{12}$ with $H = Bi_{12}(Bi/M)_4O_{14}$, $D = Bi_4(Bi/M)_4O_4$, $t = M_{x<2}$, where M stands for the divalent metal and mixed Bi/M sites denote the filled mixed Bi^{3+}/M^{2+} edges of ribbons. It will be very useful for the investigation to come to remark that two subsequent tunnels take place in the available space between one ribbon and the next ribbon-fin separated by 7.6 Å along c.

(B) New H/Qtt Structural Type. This investigation concerns a sample of composition $Bi_5Cu_2O_5(PO_4)_3$. Once more, the XRD powder pattern shows evidence of a multiphase mixture.

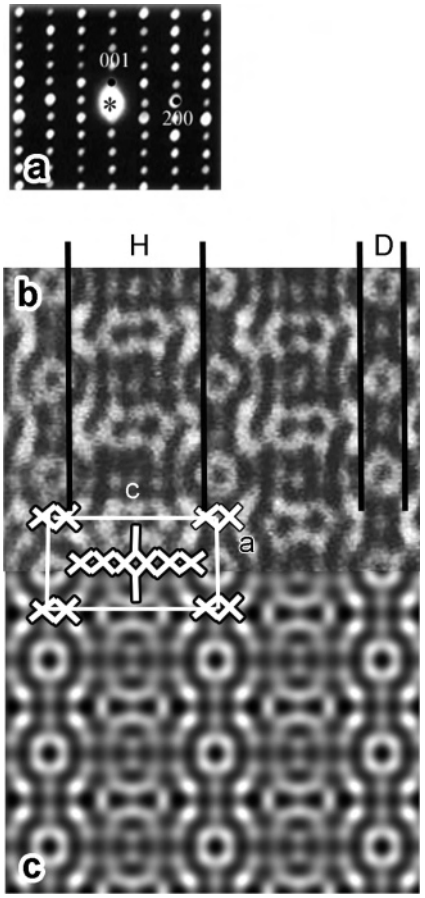

Figure 4. [010] EDP and HREM image crystallite with a Dtt/H sequence ($c \approx 21$ Å). (a) EDP; (b) experimental image: D and H columns are related to double and sextuple ribbons, which take place in the dark region along the a axis; (c) simulated image for a thickness of 4.3 nm and a defocus of −10 nm.

HREM Contrast Interpretation. The ED patterns reveal crystallites with parameters: $a \approx 11.5$ Å, $b \approx 5.5$ Å, and $c \approx 25$ Å. The [010] zone axis pattern (ZAP) is compatible with a primitive Bravais lattice. The [010] image is shown in Figure 5. The contrast is made of type H columns (white ovals surrounded by chevrons headed in the opposite direction) and a new kind of column (type Q) along a that is formed of white oval without chevron. The interpretation of the latter contrast has been logically achieved by deleting column H, the structural part that corresponds to the chevrons. This is shown in Figure 6 and leads to column Q being assigned to quadruple ribbons modified by central ribbon-fins. They take place in the dark regions of column Q, between two white ovals along the a axis. The count of the surrounding PO_4 groups around quadruple ribbons is simply deduced from the chevron removal, which transforms $H+(PO_4)_{12}$ to $Q+(PO_4)_8$ (see Figure 6). So, the structure is built on the stacking of six-tetrahedra-wide ribbons associated with ribbon-fins that are surrounded by 12 PO_4 groups and quadruple ribbons with fin surrounded by eight PO_4 groups. The estimated distance Q-fin(H) of about 8 Å (deduced from the ribbon localization) leads to the postulated H/Qtt sequence (Figure 5).

Chemical Composition. Bi coordinates for this model have been estimated by analogy to other compounds (the

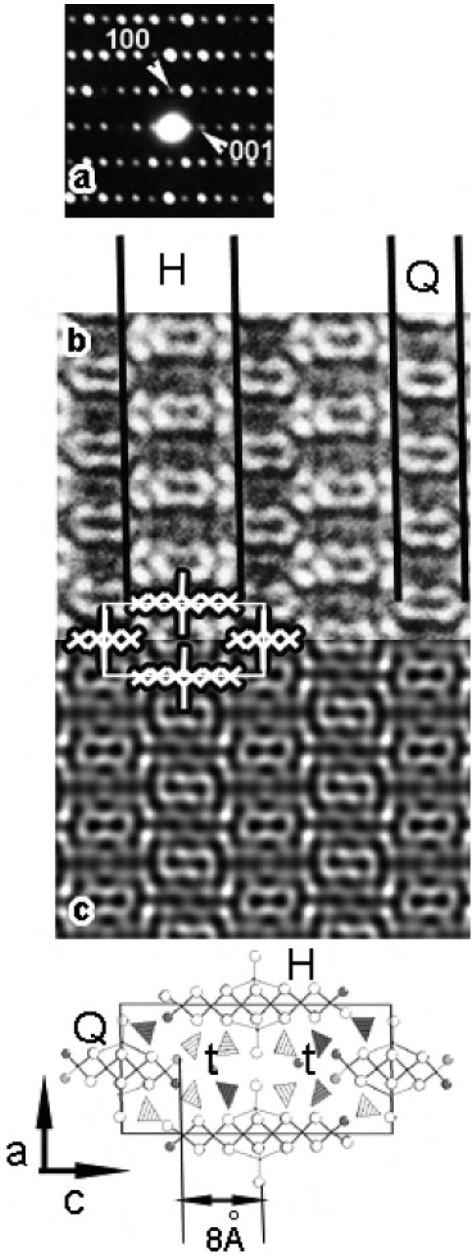

Figure 5. [010] EDP and HREM image of the H/Qtt structural type, c ≈ 25 Å. (a) EDP; (b) experimental image: H and Q columns show sextuple and quadruple ribbons, which take place in the dark regions along the *a* axis; (c) simulated image for a thickness of 4.3 nm and a defocus of −10 nm.

intraribbon structure remains nearly unchanged for all of the compounds characterized so far). From this rough model, we have simulated an image for a thickness of 4.3 nm and a defocus of −10 nm, which matches rather well with the experimental image (Figure 5). The formula deduced from the *a*,*c* projection is $H_1Q_1t_2(PO_4)_6$, where H = $Bi_{12}(Bi/M)_4O_{14}$, Q = $Bi_8(Bi/M)_4O_{10}$, and t = $M_{x<2}$. The main formula is $Bi_{20}(Bi,M)_8O_{24}(PO_4)_{12}M_{x<4}$. The validation of this formula and our postulated structural model is reported in Part 2 of our work.[18]

(**C) New tP/Pt Structural Type.** As previously described, the $BiCd_{0.29}Cu_{0.03}(PO_4)_{0.59}O_{0.93}$ preparation contains a mixture of Dtt/H-like compound and at least one unidentified additional phase. For some crystals, the parameters a ≈ 5.5 Å, b ≈ 11.5 Å, and c ≈ 25 Å are revealed by electron diffraction. Note that despite the *c* value being very close to the previous one, the symmetry indicated by the ED pattern is different. In this case, the [010] ZAP is compatible with an I Bravais lattice.

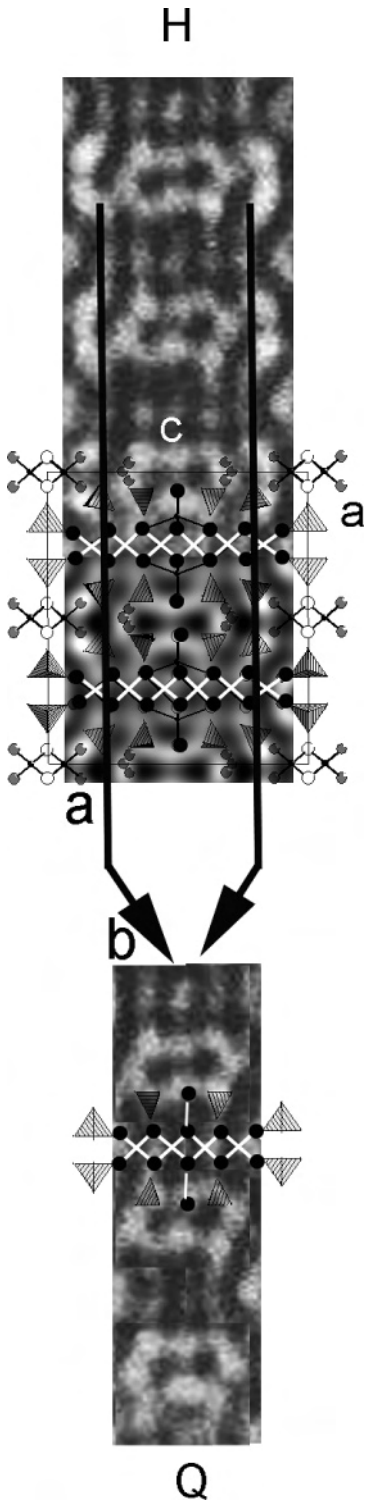

Figure 6. Structural identification of the contrast of Q columns from the H column. The removal of chevrons of H columns leads to Q columns. It leads to quadruple ribbons with central "ribbon-fins" surrounded by eight PO_4.

New P-like Ribbons and Their Interpretation. The contrast of the [010] HR image (Figure 7, image c1) consists

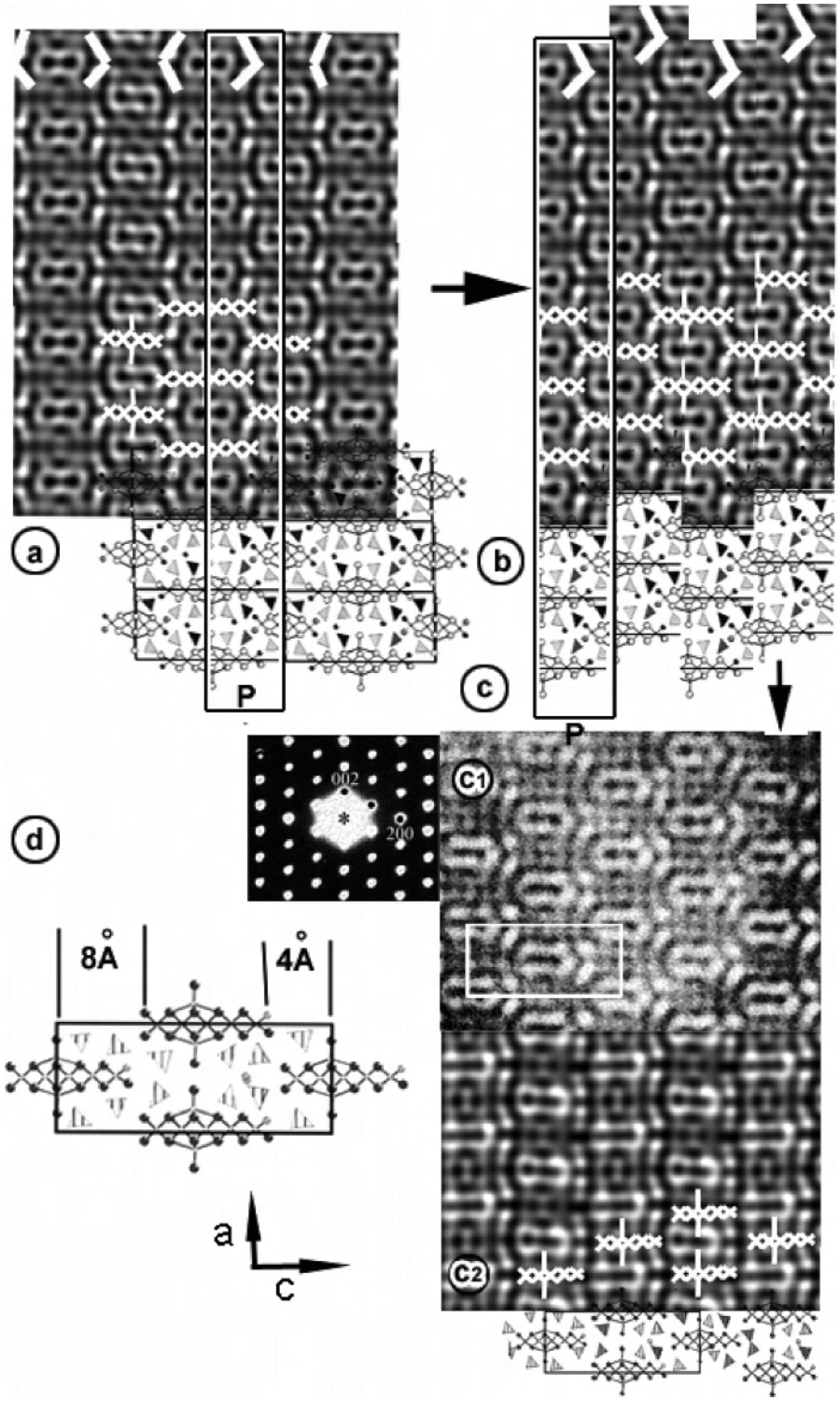

Figure 7. tP/Pt case, c ≈ 25 Å. Reconstruction of the experimental contrast of image c1 from the H/Qtt image (see Figure 6a). (a) H/Qtt: isolation of P bands consisting of ovals with chevrons in one direction and their corresponding structural projection. (b) Rearrangement of the bands by *a*/2 translation. The resulting contrast corresponds to image c1. (d) Experimentally deduced structural model. It consists of the regular alternation of five-tetrahedra-wide ribbons (═P) with an off-centered ribbon-fin. (c2) Calculated image for a defocus of −10 nm and a thickness of 3.2 nm and its corresponding projection. (c3) EDP corresponding to the experimental image of image c1.

of contrast formed of new columns called type P. They are intermediate between columns Q and H, because the central white oval shows one chevron at only one edge. Within the P columns, all the chevrons point toward the same direction. On this basis, the simple observation of the [010] HR image leads to two important structural features: the probable existence of five-tetrahedra-wide ribbons (type P for penta) intermediate between Q and H, and the likely noncentrosymmetric space group, in agreement with chevrons pointing toward the same direction.

To accurately characterize and locate the ribbons arrangement, one should notice that it is possible to reconstruct the

contrast from the image of Figure 5 (Dtt/H sequence). From this, bands consisting of white oval with chevrons in one direction and their corresponding structural projection are cut (Figure 7a) and translated from each other by *a*/2 (Figure 7b). The contrast obtained in Figure 7b corresponds to experimental image c1 on Figure 7. It yields the deduced structural model of Figure 7d. It consists of the regular alternation of penta-tetrahedral-wide ribbons, so-called P, with off-centered ribbon-fins attached between the 2nd and 3rd tetrahedral surrounded by 10 PO_4 groups. The *a*,*c* plane projection exhibits an $(a + c)/2$ translation, compatible with the I Bravais lattice.

A simple structural model that considers Bi-only cations was constructed to simulate the [010] image for a thickness of 3.2 nm and a defocus of −10 nm (Figure 7, image c2). The observed and calculated contrasts match well, in agreement with the code and model validities.

Chemical Formulation. The structural scheme proposed in the Figure 7d shows a ribbon-to-ribbon distance of about 12 Å. This distance is split in two segments of ∼8 and ∼4 Å beyond the central fin. According to previous observations, the deduced sequence is then tP/Pt. Considering the 12 PO_4 groups around H and the eight PO_4 groups surrounding Q, steric notions strongly suggest 10 PO_4 groups around P (like in the image reconstruction of Figure 7d). On the basis of the model of Figure 7d, this number is fully compatible with the four PO_4 expected to coordinate to the t tunnels. The developed formula for this new tP/Pt structural type then becomes $P_2t_2(PO_4)_{12}$, where P = $Bi_{10}(Bi/M)_4O_{12}$ and t = $M_{x<2}$. The mean formula is $Bi_{20}(Bi,M)_8$ $M_{x<4}O_{24}(PO_4)_{12}$, which reveals the isomeric character of the tP/Pt and the H/Qtt crystal types. This formula well-suits the compositional narrow zone of the various competing materials in the $Bi_2O_3-MO-P_2O_5$ phase composition diagrams, confirming the difficulty in preparing pure samples. Among a great number of pure tP/Pt material syntheses, the XRD pattern for $Bi_{20}Cd_{7.42}Cu_{0.58}O_{24}(PO_4)_{12}$ was almost fully indexed using an orthorhombic *I* unit cell with parameters $a = 11.663(8)$ Å, $b = 5.381(5)$ Å, $c = 25.066(11)$ Å. Its ab initio structural determination and refinement using SHELXS and Fullprof 2000 undoubtfully confirms the postulated structure as reported in part II.[18]

(D) Defects, H/Q/P Intergrowth. Some images from the $Bi_6Cu_2O_{12}(PO_4)_3$ study show stacking defects (black arrow in Figure 8). Outside the defect area, the contrast is made of the regular alternation of two kinds of column along *a*: a type H column of white oval surrounded by chevrons headed in the opposite direction related to sextuplet chains with fin, and a type Q column of white oval without chevron linked to quadruple ribbons with fins. Each column is translated from the other by *a*/2.

The defect consists of the deletion of an extremity of arrow in a type H column (black arrow in Figure 8). This removal is schematically represented in Figure 8 with a white line, which coincides in the structure with the suppression of one tetrahedra in the six-tetrahedra-wide chains with fin and the corresponding phosphate groups. It leads to a type P column (along *a*) that consists of five-tetrahedra-wide ribbons with an off-centering fin, as in the previous sample. On the other hand, the defect lies in the modification of the alternation. After the black arrow, a type H column is found instead of a type Q column normally expected, considering the regular alternation. In other words, we find six-tetrahedra-wide chains with fins instead of four-tetrahedra-wide ribbons with fins. A model of the local defect can be proposed that leads to a type P column (five-tetrahedra-wide ribbons with decentered fins) followed by a type H column (six-tetrahedra-wide chains with fins); see Figure 8. Each column is translated from the other by *a*/2.

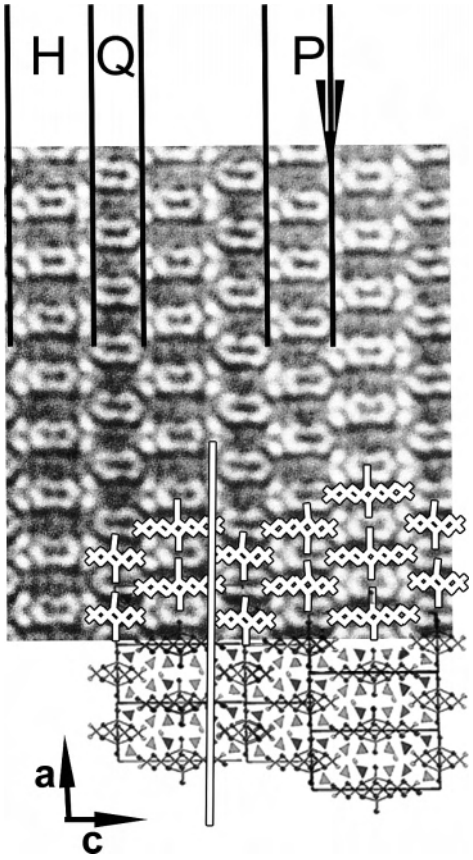

Figure 8. Defects in the H/Qtt structure shown by the black arrow ($Bi_{20}Cd_{7.42}Cu_{0.58}O_{24}(PO_4)_{12}$ sample). The observed defects consist of the deletion of one row of chevrons from the H column, leading to a P-type column (5 tetrahedra wide). The original H/Q arrangement is modified to a P/Q arrangement.

Concluding Remarks

In a previous work, the possibility of assigning a structural type to the [010] HREM images of Bi^{3+}/M^{2+} oxyphosphates was shown. This property is due to the particular structure of these compounds built from isolated 2D polycationic ribbons with variable width. So far, the size of the observed ribbons was limited to a width of $n = 3$ $O(Bi,M)_4$ tetrahedra. Herein, new HREM contrasts observed in inhomogeneous samples have been assigned to the $n = 4-6$ cases, leading to the postulation of three new structural types. The electron microscope investigation then enables the general formulation corresponding to the depicted structure using empirical rules deduced from the examination of other compounds within these series. The validity of our investigation has to be

checked by structural proof. This stage is presented in Part 2 of our work. Finally, according to the number of polycations ($n = 1,2, ..., 6$) discovered so far and their various arrangements together via phosphates, this work shows the rich character of $Bi_2O_3-MO-P_2O_5$ ternary diagrams and strongly suggests an unlimited number of possible original materials.

Acknowledgment. M. Colmont thanks the Région-Nord-Pas-de-Calais for financial support. The authors sincerely thank the EMAT laboratory (Antwerp, Belgium) for microscopy facilities.

IC060342R